

# An Adaptive Supplementary Controller for a UPFC

Urvi Malhotra, Ramakrishna Gokaraju, Dharshana Muthumuni

**Abstract**— In this paper, a supplementary adaptive controller consisting of a Constrained Recursive Least Squares (CRLS) online identifier and a Pole Shift (PS) controller for a UPFC is presented. The goal of the adaptive controller is to supplement the conventional Proportional-Integral (PI) based UPFC control system in damping low frequency power oscillations during major disturbances or faults. PI controllers are fixed-parameter based controllers that are tuned for a particular operating point and are incapable of adapting to the system changes, unless re-tuned through external operator intervention. In order to overcome this problem, in this work, the PI controllers are provided with an adaptive supplementary controller that tracks the system changes online through its CRLS identifier and also eliminates the effort of manual parameter re-tuning through its PS control algorithm. In order to correctly identify the system parameters especially during large disturbances such as three-phase faults, a constrained RLS identification technique is implemented. The effectiveness of the proposed method has been demonstrated in a two-area test power system where its performance in damping power oscillations is compared to a conventional PI-controlled UPFC control system.

**Keywords:** FACTS, UPFC, power oscillation damping, adaptive control.

## I. INTRODUCTION

LOW frequency inter-area power oscillations in the range of 0.1 to 0.8 Hz are often observed when power systems are interconnected through relatively weak tie lines [1] and are subjected to disturbances such as faults or line outages. The advent of different Flexible AC Transmission Systems (FACTS)-based devices for transmission paths have provided the capability of controlling the bus voltages and power flows to a desired level and also enhancing the damping of power oscillations. The Unified Power Flow Controller (UPFC), proposed by Gyugyi in 1991 [2], is a versatile FACTS –based device that has the unique capability of controlling both-the real and reactive power flow while maintaining a constant bus voltage at its point of installation. In addition to the power and voltage control, the efficacy of a UPFC in damping power oscillations has been previously demonstrated [3]-[5] through the design of a suitable control system. One of the most common and suited design approaches has been to use PI control loops. The conventional PI controllers are simple to implement and are very effective in damping oscillations

when tuned for a particular operating condition. However, unless manually re-tuned, they suffer from the inadequacy of suitable control and transient stability enhancement over a wide operating range. It is a known fact that a power system’s operating point continually changes over time with changes in system configuration, generation, load or faults. So, repeated tuning of PI controllers is inadvisable. For this reason, it is desirable to develop controllers that are impervious to changes in operating conditions and thereby eliminate the need of offline parameter tuning. Adaptive controllers are preferred under such circumstances that are capable of adapting to the new operating condition in real-time and thereby yielding optimum response over wide operating regions.

In this paper, authors propose the use of an adaptive controller comprising of the CRLS identifier algorithm and the PS control algorithm that is installed as a supplementary controller to the PI-controlled UPFC control system. The proposed adaptive controller has the advantages of being self-tuned, offers rapid parameter tracking and is independent of manual or offline re-tuning. Additionally, a constrained-parameter tracking approach by the RLS identifier makes the identification stable and yields a smooth parameter variation especially for large disturbances.

The paper is organized as follows. Section II provides a brief discussion on the functionality of the UPFC and describes a control system model that includes the proposed adaptive controller. Section III gives a description of the supplementary adaptive control technique proposed here. The electromagnetic transient simulation results considering a two-area test system subjected to different power flows and fault conditions are presented in Section IV. This is followed by presentation of conclusions in Section V.

## II. UPFC IN DAMPING POWER OSCILLATIONS

The basic arrangement of a UPFC installed between the sending end bus,  $s$  and the receiving end bus,  $r$  is shown in Fig. 1.

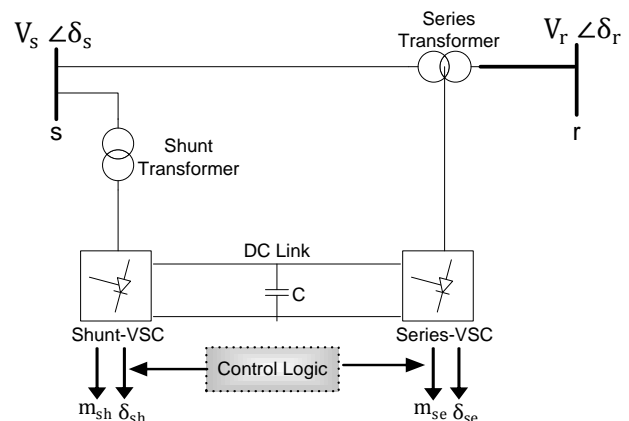


Fig. 1. Circuit arrangement for a UPFC installed between buses  $s$  and  $r$ .

U. Malhotra and R. Gokaraju are with the Department of Electrical and Computer Engineering, University of Saskatchewan, Saskatoon, SK S7N 5A9 Canada (e-mail: [urml52@mail.usask.ca](mailto:urml52@mail.usask.ca) and [rama.krishna@usask.ca](mailto:rama.krishna@usask.ca)).

D. Muthumuni is with Manitoba HVDC Research Center, Winnipeg, MN R3P 1A3 Canada (e-mail: [dharsana@hvdc.ca](mailto:dharsana@hvdc.ca)).

Paper submitted to the International Conference on Power Systems Transients (IPST2011) in Delft, the Netherlands June 14-17, 2011

This UPFC model is based on the Voltage Sourced Converter (VSC) topology. A UPFC consists of a shunt-VSC and a series-VSC connected to the power system buses through a shunt and a series transformer respectively. The VSCs are mutually connected together through a common DC link supported by a DC capacitor,  $C$ . Each converter typically consists of six thyristor valves. The converter operations are governed by a pair of two control inputs. Each input pair comprises of a modulation ratio and phase angle order inputs. The injected shunt current by the shunt-VSC is controlled by its modulation ratio,  $m_{sh}$  and phase angle order,  $\delta_{sh}$ . The series injected voltage, decided by the series-VSC is controlled by a modulation ratio,  $m_{se}$  and a phase angle order,  $\delta_{se}$ . Achieving a desired steady-state power flow on a particular transmission line controlled by the UPFC corresponds to obtaining steady-state values of the four control inputs of the UPFC. The primary purpose of controlling real and reactive power flow over transmission line is met by the series converter. It injects a voltage,  $V_{inj}$  in series with the line reactance at fundamental frequency that is controllable both in magnitude ( $0 \leq |V_{inj}| \leq V_{max}$ ) and in phase ( $0 \leq \delta_{inj} \leq 360^\circ$ ). On the other hand, the purpose of the shunt converter is to provide the real power drawn by the series branch by maintaining a constant DC link voltage that is decided by the system configuration and device ratings. Additionally, the shunt converter can also independently provide reactive power support to the shunt bus to which it is connected.

To meet the objective of damping power system oscillations, the design of a suitable UPFC control system is essential. Also, the control input signals should be readily and locally available to avoid the need of communication channels for long-distance data transmission and delayed controller responses. Since the UPFC is devised for transmission control, locally available signals such as bus voltages and current/power flows are the preferred control inputs. UPFC's control system is based on the design of a shunt and series control system for its shunt and series converters respectively. Fig. 2 gives the block diagram representation of the shunt converter's control system. The shunt converter control scheme discussed here is based on the *Automatic Voltage Control Mode* that aims at controlling the sending-end bus voltage magnitude and the DC link voltage magnitude. It thus consists of two PI control loops. The off-nominal PI parameters selected to demonstrate the effectiveness of the adaptive controller are given in Table 2.

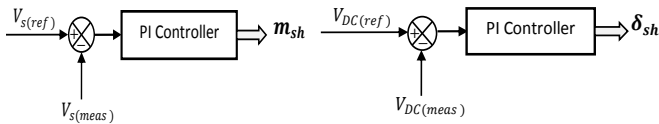


Fig. 2. Shunt converter control system using conventional PI controllers

The DC link voltage magnitude,  $V_{DC}$  is chosen as the control input to modulate the shunt converter's phase angle order,  $\delta_{sh}$ . The phase shift,  $\delta_{sh}$  introduced by this converter facilitates

transfer of real power to or from the DC link in order to meet the real power demand by the series converter. Also, the sending-end bus voltage,  $V_s$  is selected as the control input to adjust converter's modulation ratio,  $m_{sh}$  so as to regulate the bus voltage to 1 p.u.

Fig. 3 illustrates the block diagram of the series converter's control system. To focus on damping oscillations, control of series injected voltage by the series-VSC is considered for damping control. In Fig. 3, PI-type controllers control the series injected voltage during transient conditions.

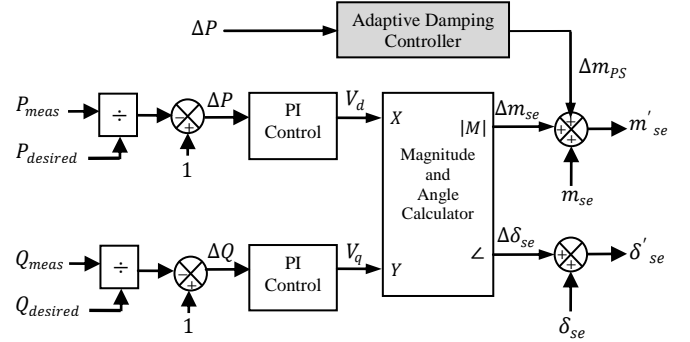


Fig. 3. Series converter control system using conventional PI controllers

Further damping enhancement is accomplished by adding a damping signal through a supplementary control loop provided by the adaptive controller. The control system model is based on the *Automatic Power Flow Control Mode*. In this mode, the amount of series injected voltage is directly governed by the desired real and reactive power flows on the tie network. The control inputs are the directly measurable real and reactive power flows on the tie line. The steady-state values of the converter's modulation ratio,  $m_{se}$  and phase angle order,  $\delta_{se}$  are pre-calculated depending on the desired real and reactive power flows needed during non-faulted conditions. The control strategy [6] works in such a way that the desired active power,  $P_{desired}$  and reactive power  $Q_{desired}$  are compared with the measured active power,  $P_{meas}$  and reactive power,  $Q_{meas}$  and the errors are passed through corresponding PI controllers which produce the direct ( $V_d$ ) and quadrature ( $V_q$ ) components of the series-connected compensating voltage. A magnitude-angle calculator block converts the series voltage (d-q frame) to the corresponding damping inputs  $\Delta m_{se}$  and  $\Delta \delta_{se}$  respectively.

A PI-control based UPFC damping model is supplemented with an adaptive controller to enhance the damping capability during severe faults or line outages. Oscillations in power flow can be effectively damped out by corresponding modulations in the real and reactive power flows. This, in turn, is achieved by suitably varying the modulation ratio of the series converter,  $m_{se}$ . Hence, the control input to the adaptive damping controller is the deviation in the real power flow,  $\Delta P$ . The controller generates the extra damping control signal,  $\Delta m_{PS}$  as its output. The overall damping provided by the series converter essentially depends on the total modulation ratio,  $m'_{se}$  ( $m_{se} + \Delta m_{se} + \Delta m_{PS}$ ) and phase angle order,  $\delta'_{se}$  ( $\delta_{se} + \Delta \delta_{se}$ ).

### III. SUPPLEMENTARY ADAPTIVE CONTROLLER

The principle of adaptive control is based on self-tuning control as shown in Fig. 4. In this approach, first, the power system including the UPFC is represented by a suitable fixed-order mathematical (ARMA) model. Next, an identifier is used to determine the parameters of the ARMA model. Finally, the updated parameters that track the system operating conditions are used by the pole-shift controller to compute the necessary control. The computation of the updated parameters and control is done on-line every sampling period.

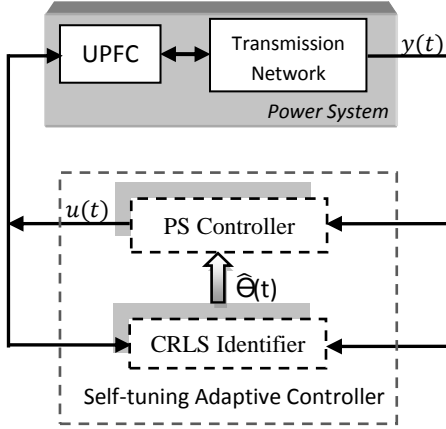


Fig 4. Self-tuning adaptive control

#### A. CRLS Identifier

The procedure of system identification is based on parameter estimates that should, ideally, identically represent the plant's behavior even during disturbances. This is made possible by recursively calculating the plant parameters at a pre-defined sampling rate. A commonly used technique of achieving a continuous closed-loop tracking of the system's behavior is the recursive least squares parameter identification method. Additionally, to enhance the ability of the identifier to track actual system conditions and to avoid the parameter burst-out, a forgetting factor is used to discount the importance of the older data [7]. Further, to correctly estimate the system parameters during large disturbance such as three-phase faults, a constrained-RLS approach is used that provides a smooth parameter variation. It prevents a noisy controller output during initial swings following a disturbance. The CRLS identification algorithm approximates the dynamics of the power system accompanied by a UPFC through a discrete ARMA model given by:

$$A(z^{-1})y(t) = B(z^{-1})u(t) + e(t) \quad (1)$$

where  $y(t)$ ,  $u(t)$  and  $e(t)$  are the system output, input and noise terms respectively.  $A(z^{-1})$ ,  $B(z^{-1})$  and  $C(z^{-1})$  are the polynomials expressed in terms of the backward shift operator  $z^{-1}$  and are defined as:

$$\begin{aligned} A(z^{-1}) &= 1 + a_1 z^{-1} + a_2 z^{-2} + \dots + a_{n_a} z^{-n_a} \\ B(z^{-1}) &= b_1 z^{-1} + b_2 z^{-2} + \dots + b_{n_b} z^{-n_b} \end{aligned} \quad (2)$$

$n_a$  and  $n_b$  are the orders of the polynomials  $A(z^{-1})$  and  $B(z^{-1})$  respectively. Re-writing Equation (1) in the following form suitable for identification [7]:

$$y(t) = \hat{\theta}^T(t)\phi(t) + e(t) \quad (3)$$

where  $\hat{\theta}^T(t) = [a_1 \ a_2 \ a_3 \ \dots \ a_{n_a} \ b_1 \ b_2 \ b_3 \ \dots \ b_{n_b}]^T$  is the system parameter vector,  $\phi(t) = [-y(t-1) \ -y(t-2) \ \dots \ -y(t-n_a) \ u(t-1) \ \dots \ u(t-n_b)]$  is the sampled input/output measurement data vector and  $e(t)$  is the measurement white noise. Then, the CRLS algorithm that includes a variable forgetting factor,  $\rho(t)$  and the tracking constraint term,  $\beta(t)$  given in (4) can be used to identify the system parameter vector  $\hat{\theta}^T(t)$  as [8]:

$$\begin{aligned} \hat{\theta}^T(t+1) &= \hat{\theta}^T(t) + K(t) [y(t) - \hat{\theta}^T(t)\phi(t)]\beta(t) \\ K(t) &= \frac{P(t)\phi(t)}{\rho(t) + \phi^T(t)P(t)\phi(t)} \\ P(t+1) &= \frac{1}{\rho(t)} [P(t) - K^T(t)P(t)\phi(t)] \end{aligned} \quad (4)$$

$$\rho(t) = \rho_0 \rho(t-1) + (1 - \rho_0)$$

where  $\rho_0$  is a positive value between 0 and 1,  $P(t)$  is the error covariance matrix and  $K(t)$  is the modifying gain matrix.  $\beta(t)$  is calculated at each sampling interval as:

$$\begin{aligned} \beta(t) &= 1.0 && \text{if } \frac{N_2}{N_1} \leq \beta_0 \\ &= 1.0 \frac{\beta_0}{N_2} && \text{if } \frac{N_2}{N_1} > \beta_0 \end{aligned} \quad (5)$$

where

$$\begin{aligned} N_1 &= \|\hat{\theta}(t)\|_2 \\ N_2 &= \|K(t) [y(t) - \hat{\theta}^T(t)\phi(t)]\|_2 \end{aligned}$$

$\|\cdot\|$  is the norm of the corresponding vector, and  $\beta_0$  is a positive constant to determine the updating rate of the identified parameters.

#### B. Pole-shift (PS) control concept

The concept of the PS control is based on the Minimum Variance (MV) control and the Pole Assignment (PA) control. Similar to the PA controller, the PS controller emphasizes on the closed-loop stability by self-searching a single pole shifting factor,  $\alpha$  obtained by minimization of a suitable performance index at each sampling instant. The performance index is based on the minimum variance criterion. Also, to ensure closed-loop stability at all times, the closed-loop poles are restricted to lie within the unit circle in the  $z$ -domain. The

closed loop system configuration with the PS controller in the feedback loop is shown in Fig. 5. The PS controller assumes the feedback loop of the form:

$$\frac{u(t)}{y(t)} = -\frac{G(z^{-1})}{F(z^{-1})} \quad (6)$$

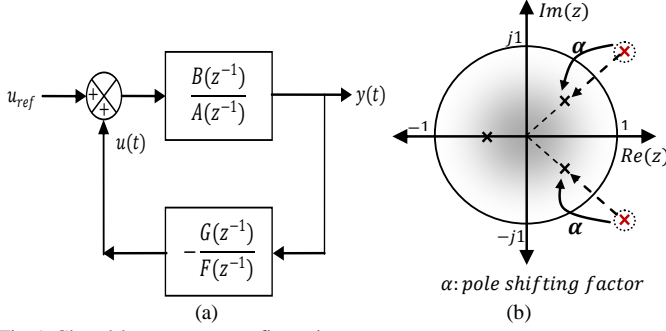


Fig 5. Closed-loop system configuration

where,

$$F(z^{-1}) = 1 + f_1 z^{-1} + f_2 z^{-2} + \dots + f_{n_f} z^{-n_f}$$

$$G(z^{-1}) = g_0 + g_1 z^{-1} + g_2 z^{-2} + \dots + g_{n_g} z^{-n_g}$$

and  $n_f = n_b - 1$ ,  $n_g = n_a - 1$ . From (1) and (6) and from Fig. 5, the characteristic equation of the closed loop control is:

$$T(z^{-1}) = A(z^{-1})F(z^{-1}) + B(z^{-1})G(z^{-1}) = 0 \quad (7)$$

The PS algorithm shifts the open-loop poles by the same factor,  $\alpha$  and the closed-loop characteristic polynomial takes the following form:

$$A(z^{-1})F(z^{-1}) + B(z^{-1})G(z^{-1}) = A(\alpha z^{-1}) \quad (8)$$

In the PS algorithm,  $\alpha$ , a scalar, is the only parameter to be determined and its value reflects the stability of the closed-loop system [9]. The pole-shifting process is schematically shown in Fig. 5(b).

Re-arranging (6) in matrix form gives:

$$\begin{bmatrix} 1 & 0 & \dots & 0 & b_1 & 0 & \dots & 0 \\ a_1 & 1 & \dots & 0 & b_2 & b_1 & \dots & 0 \\ \vdots & \vdots & \ddots & \vdots & \vdots & \vdots & \ddots & \vdots \\ a_{n_a} & a_{n_a-1} & \dots & 1 & b_{n_b} & b_{n_b-1} & \dots & b_1 \\ 0 & a_{n_a} & \dots & a_1 & 0 & b_{n_b} & \dots & b_2 \\ 0 & 0 & \dots & a_2 & 0 & 0 & \dots & b_3 \\ \vdots & \vdots & \ddots & \vdots & \vdots & \vdots & \ddots & \vdots \\ 0 & 0 & \dots & a_{n_a} & 0 & 0 & \dots & b_{n_b} \end{bmatrix} \begin{bmatrix} f_1 \\ \vdots \\ f_{n_f} \\ g_0 \\ \vdots \\ g_{n_g} \end{bmatrix} = \begin{bmatrix} (\alpha - 1)a_1 \\ (\alpha^2 - 1)a_2 \\ \vdots \\ (\alpha^{n_a} - 1)a_{n_a} \\ 0 \\ \vdots \\ 0 \end{bmatrix}$$

or,

$$M \cdot (\alpha) = L(\alpha) \quad (9)$$

where the elements of matrix  $M$  are the parameters  $\{a_i\}, \{b_i\}$  that are identified by the identifier every sampling period. If the value of pole shift factor,  $\alpha$ , is known, (9) can be solved for the control parameters  $\{f_i\}$  and  $\{g_i\}$  following which control output,  $u(t)$  can be obtained using (6). Since the

essence of pole shift algorithm is based on  $\alpha$ , for optimum performance, it is desirable to obtain the value of  $\alpha$  online and at each sampling instant. Pole shift factor,  $\alpha$  is selected so as to optimize certain performance index,  $J(t + 1, \alpha_t)$ . Here,  $\alpha$  is calculated iteratively to minimize the one time-step ahead prediction error in  $y(t)$ , i.e.

$$\min_{\alpha_t} J(t + 1, \alpha_t) = E[\hat{y}(t + 1) - y_r(t + 1)]^2 \quad (10)$$

where  $E$  is the expectation operator,  $\hat{y}(t + 1)$  is predicted output and  $y_r(t + 1)$  is the reference value. The predicted output  $\hat{y}(t + 1)$  can be calculated as

$$\hat{y}(t + 1) = X^T(t)\beta + b_1[u(t, \alpha_t)] \quad (11)$$

where,

$$X(t) = [-u(t - 1) \dots - u(t - n_f) - y(t) - y(t - 1) \dots - y(t - n_g)]^T \text{ and } \beta = [-b_2 - b_3 \dots - b_{n_b} \ a_1 \ a_2 \ \dots \ a_{n_a}]^T.$$

The minimization function in (10) is a constrained optimization routine subjected to a *stability* constraint and a *control* constraint. The *stability* constraint defines the range of  $\alpha_t$  to be within  $(\frac{-1}{\lambda}, \frac{1}{\lambda})$ , where  $\lambda$  represents the absolute value of the largest root of the characteristic equation  $T(z^{-1})$ . Further, the *control* constraint emphasizes on the control signal to lie within the controllable range,  $(u_{min}, u_{max})$ , where  $u_{min}$  and  $u_{max}$  are the minimum and maximum control signal boundaries respectively. For the UPFC application, this controllable range is decided by the minimum and maximum series voltage injection available by the series-VSC which in turn depends on the compensation range provided by the series-VSC.

#### IV. SIMULATION RESULTS

To validate the performance of the proposed adaptive supplementary controller, the Kundur's four-machine two-area test power system shown in Fig. 6 is considered. The system has one inter-area mode with poor damping. The PI controllers are initially tuned to achieve a power flow of 400MW from Area 1 to Area 2. The robustness of the proposed controller in damping inter-area oscillations is demonstrated by subjecting the test system to different transient disturbances.

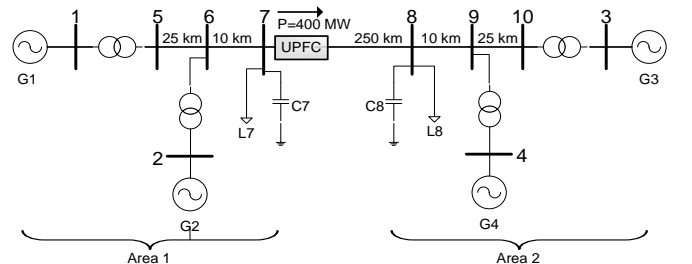


Fig 6: Kundur's Two-Area Test System including a UPFC at bus 7.

The details of multi-machine system configuration are given in [10] and the UPFC's steady-state control inputs  $m_{sh}$ ,  $\delta_{sh}$ ,  $m_{se}$  and  $\delta_{se}$  are given in Appendix. The UPFC is assumed to compensate for 20% of the impedance of the line 7 – 8. The plant dynamics is approximated by a third-order ARMA model. The third order model is sufficient to represent the plant dynamics having one oscillating component and one decaying component [11]. Through load flow analysis for a desired power flow of  $P_{7-8} = 400MW$ , bus 7 refers to the bus with the weakest voltage profile ( $< 0.96 p.u.$ ). Hence, the shunt-VSC of the UPFC is connected to bus 7. Also, in order to maintain a desired inter-area power flow, the UPFC is installed at the sending end of Area 1 i.e. at bus 7 for all the case studies. To meet the objective of enhancing damping of power oscillations, the supplementary controller considers the real power flow deviation at bus 7,  $\Delta P_7$  as its control input. The input signal is sampled with a  $50ms$  sampling period. It is important that the power system including the UPFC must obey the following two objectives:

*Steady-state control:* In steady-state, the UPFC must establish a desired power flow from Area 1 to Area 2 by injection of a suitable series three-phase voltage. This corresponds to specific values of the series-VSC control parameters,  $m_{se}$  and  $\delta_{se}$  during non-disturbed condition. The shunt-VSC, in addition to regulating the DC link voltage,  $V_{DC}$  to a pre-specified value, must also be capable of maintaining a constant bus voltage at bus 7.

*Transient control:* In this operating region, the supplementary adaptive controller must improve the existing damping originally provided by the UPFC's PI-control system for off-nominal PI parameters. The off-nominal state represents those system conditions when the PI-parameters are not re-tuned and are thus non-optimal. However, an acceptable damping performance is still achievable due to the presence of the supplementary controller.

The performance of the proposed controller is shown under the following test conditions.

#### A. Three-phase to ground fault

A three-phase to ground fault of  $50ms$  duration is simulated at Bus 8 for a  $400MW$  of real power transfer from Area 1 to Area 2. Fig. 7 shows the comparison of the conventional PI controller (*dotted line*) and the proposed controller (*bold line*). The performance of the supplementary controller with the CRLS identifier is notably superior in comparison to using only the PI controller. The control effort initiated by the adaptive controller along with the corresponding pole shift factor variation,  $\alpha_t$  are shown in Fig. 8.

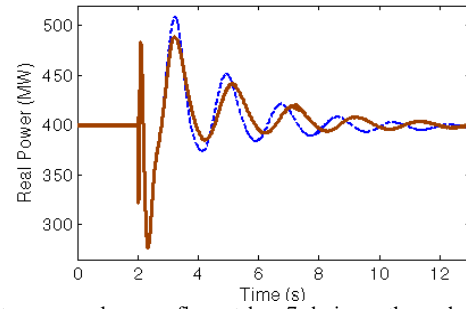
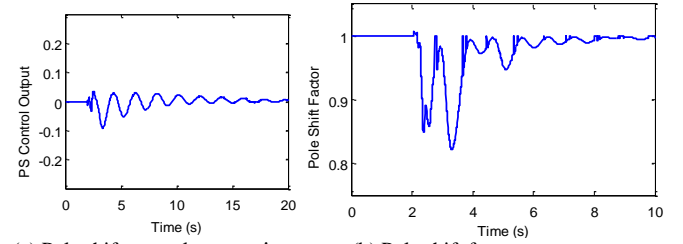


Fig. 7. Inter-area real power flow at bus 7 during a three-phase to ground fault at bus 8.



(a) Pole shift control output,  $\Delta m_{p5}$  (b) Pole shift factor,  $\alpha_t$   
Fig. 8. Supplementary adaptive controller action

The RLS identifier accompanied by the constrained coefficient  $\beta$  provides a smooth parameter variation even during the severe fault condition. The parameter tracking capability is illustrated in Fig. 9. The variation of the voltage across the DC capacitor is shown in Fig. 10 and it is seen that the overshoots and the settling time are well controlled by the proposed controller. The UPFC is capable of not only damping the inter-area power oscillation but also maintaining the shunt bus voltage to a fairly constant value within the acceptable range. In addition to this, the UPFC is successful in providing the real power demand to the series converter by keeping the DC link voltage to a constant value of  $42.4kV$ .

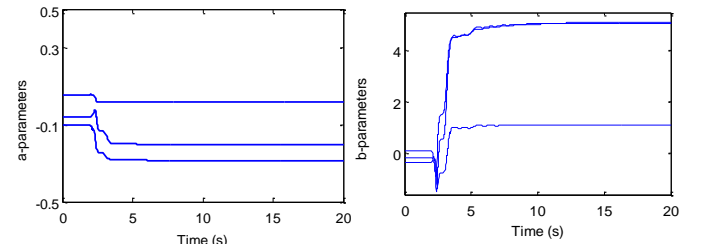


Fig. 9. Identified system parameters using constrained recursive least squares identifier (CRLS)

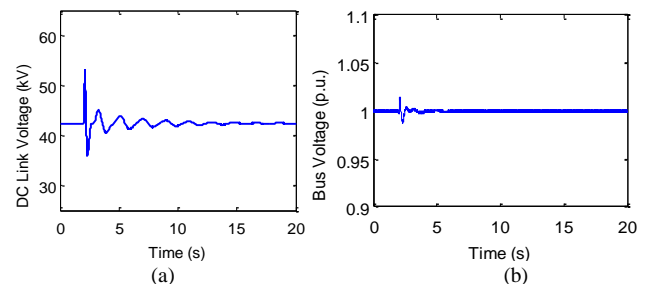


Fig. 9. (a) DC link voltage,  $V_{DC}$  across the DC capacitor and (b) Bus voltage,  $V_7$  in p.u. at UPFC location.

### B. Single-phase to ground fault

With the same operating condition as in sub-section A, the power system is subjected to a single-phase to ground fault at Bus 7 for 100 ms. Fig. 10 represents the performance of the supplementary controller (*bold line*) to be significant in damping the inter-area mode of oscillation between Area 1 and Area 2 where the PI controller response is represented by the *dotted line*. From the response it is evident that the proposed controller performs significantly in damping out power oscillations between the tie-line.

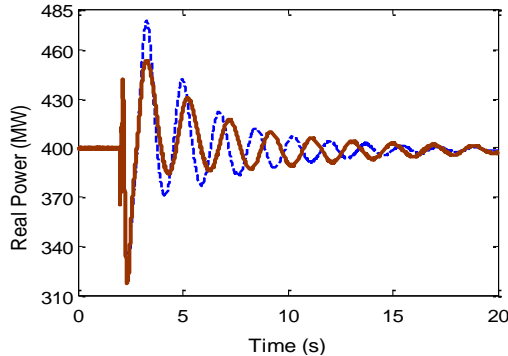


Fig. 10. Real power flow (Area 1 to Area 2) at bus 7 for a single-phase to ground fault at bus 7.

### V. CONCLUSIONS

The paper proposed the use of an adaptive supplementary controller in assisting the PI-controlled UPFC control system to damp power oscillations. In addition, the constrained recursive least squares (CRLS) identification method proved beneficial by avoiding large identified parameter variations during large system disturbances. The adaptive control scheme is discussed in detail and its favorable influence on damping oscillations is shown through electromagnetic time domain simulation analyses. The PS algorithm is self-tuned online by a single parameter to obtain an improved damping response and hence can be easily implemented in real time. The results clearly showed that adding the supplementary pole-shift control greatly enhanced the damping of inter-area power oscillation while being robust to fault types and operating conditions.

### VI. APPENDIX

The UPFC parameters and the conventional PI controller gains and time constants are given below:

TABLE I  
UPFC DESIGN PARAMETERS

UPFC compensation	20% of $X_{7-8}$
$C_{UPFC}$	15mF
$V_{7(ref)}$	1 p.u.
$V_{DC(ref)}$	42.4 kV
$m_{sh}$	0.94
$\delta_{sh}$	3.08°
$m_{se}$	0.52
$\delta_{se}$	104°

TABLE II  
OFF-NOMINAL PI PARAMETERS

$P_{7-8} = 400MW$	$K_p = 0.02$
	$T_i = 0.63$

### VII. REFERENCES

- [1] M. Klein, G. Rogers, and P. Kundur, "A fundamental study of inter-area oscillations in power systems," *IEEE Trans. Power Systems*, vol. 6, pp. 124–136, Aug. 1991.
- [2] L. Gyugyi, C. D. Schauder, S. L. Williams, T. R. Rietman, D. R. Torgerson, and A. Edris, "The unified power flow controller: A new approach to power transmission control," *IEEE Trans. Power Delivery*, vol.10, no.2, pp1085-1097, Apr. 1995.
- [3] M. Nomoian, L. Angquist, M. Ghandari and G. Anderson, "Improving Power System Dynamics by series-connected FACTS devices," *IEEE Trans. Power Delivery*, vol. 12, no. 4, pp.1635-1641, 1997.
- [4] M. Namarian and G. Anderson, "Damping of power System by controllable components," *IEEE Trans. Power Delivery*, vol. 9, pp. 2046-2054, 1994.
- [5] K. R. Padiyar and A. M. Kulkarni, "Control design and simulation of unified power flow controller," *IEEE Trans. Power Delivery*, vol. 13, no. 4, pp. 1348-1354, 1998.
- [6] K. K. Sen and M. L. Sen, "Introduction to FACTS controllers: theory, modeling and applications," New Jersey: Wiley-IEEE Press, 2009, p. 298.
- [7] G. P. Chen, O. P. Malik, G. S. Hope, Y. H. Qin and G. Y. Xu, "An adaptive power system stabilizer based on the self-optimizing pole shift control strategy," *IEEE Trans. Energy Conversion*, vol. 8, no. 4, pp. 639-645, 1993.
- [8] K. J. Åström and B. Wittenmark, "Adaptive Control", Addison-Wesley Publishing, 1989, p. 409.
- [9] G. Ramakrishna and O. P. Malik, "Radial basis function identifier and pole-shifting controller for power system stabilizer application," *IEEE Trans. Energy Conversion*, vol. 19, no. 4, pp. 663–670, Dec 2004.
- [10] P. Kundur, "Power System Stability and Control," New York: McGraw-Hill, 1994, p. 814.
- [11] O. P. Malik, G. P. Chen, G. S. Hope, Y. H. Qin, and G. Y. Xu, "Adaptive self-optimising pole shifting control algorithm," *IEE Proceedings D Control Theory and Applications*, vol. 139, no. 5, pp. 429–438, 1992.